Talanta 93 (2012) 320–325

Contents lists available at SciVerse ScienceDirect

Talanta

journal homepage: www.elsevier.com/locate/talanta

# Simultaneous electrochemical determination of uric acid, xanthine and hypoxanthine based on poly(L-arginine)/graphene composite film modified electrode

Fengyuan Zhang, Zaihua Wang, Yuzhen Zhang, Zhixiang Zheng, Chunming Wang*, Yongling Du, Weichun Ye

*Department of Chemistry, Lanzhou University, Lanzhou 730000, PR China*

ARTICLE INFO

*Article history:*
Received 31 December 2011
Received in revised form 9 February 2012
Accepted 17 February 2012
Available online 22 February 2012

*Keywords:*
Graphene
Poly(L-arginine)
Uric acid
Xanthine
Hypoxanthine

ABSTRACT

Poly(L-arginine)/graphene composite film modified electrode was successfully prepared via a facile one-step electrochemical method and used for simultaneous determination of uric acid (UA), xanthine (XA) and hypoxanthine (HX). The electrochemical behaviors of UA, XA and HX at the modified electrode were studied by cyclic voltammetry and differential pulse voltammetry (DPV), and showed that the modified electrode exhibited excellent electrocatalytic activity toward the oxidation of the three compounds. The calibration curves for UA, XA and HX were obtained over the range of 0.10–10.0, 0.10–10.0 and 0.20–20.0 μM by DPV, respectively and the detection limits for UA, XA and HX were 0.05, 0.05 and 0.10 μM (S/N = 3), respectively. With good selectivity and high sensitivity, the modified electrode has been applied to simultaneous determination of UA, XA and HX in human urine with satisfactory result.



## 1. Introduction

Uric acid (UA), xanthine (XA) and hypoxanthine (HX) are degradation products of purine metabolism in animals. Purine metabolites pathway involves transformation of HX → XA, XA → UA by xanthine oxidase, so XA and HX are intermediates and UA is the terminal product of purine degradation metabolism [1]. Abnormalities of the metabolites concentrations in body fluids such as human serum and urine are sensitive indicators of many pathologic states, including perinatal asphyxia, xanthinuria, hyperuricemia, gout, hence accurate detection and quantification of UA, XA, and HX in body fluids are critically important in study of the homeostasis of the xanthine oxidase system and clinical diagnosis at early stages of related diseases [2].

Various techniques have been developed to simultaneously determine the purine degradation products, such as enzymatic methods [3,4], high-performance liquid chromatography (HPLC) [5–7], capillary electrophoresis (CE) [8–10] and electrochemistry [11–16]. However, HPLC method is time-consuming and requires fastidious sample preparation and expensive material, CE method needs expensive apparatus, and enzymatic method is lack of stability, which hampers their further applications. Compared with these methods, simple enzyme-free electrochemical methods may be a good alternative due to their simplicity, rapid response and low cost. Actually, many efforts have been paid to develop non-enzymatic electrodes, for instance, electrodes modified with preanodized nontronite [13], carbon nanotube [14], $Ru(DMSO)_4Cl_2$ nano-aggregated Nafion membrane [15] and polymer film [17,18]. However, most of these non-enzymatic electrodes have displayed the drawbacks of high cost of rare metal precursors, low sensitivity and narrow linear range. Therefore, the development of a cheap, sensitive and interference free electrode for simultaneous determination of UA, XA and HX is still greatly demanded.

Graphene, one-atom-thick 2D layers of $sp^2$-bonded carbon has been widely explored in recent years because of their intriguing properties such as large surface areas, high electrical conductivity, flexibility, and chemical inertness [19–22]. Graphene has been obtained so far by several techniques: mechanical cleavage of graphite [22], epitaxial growth on single crystal silicone carbide as well as metals [23], thermal expansion of graphite [24], and chemical reduction of graphene oxide (GO) [25,26]. Recently, electrochemical reduction of GO to produce graphene has attracted a strong attention since it can be performed at room temperature without any dangerous chemicals [27,28]. Poly(L-arginine) (poly(L-Arg)) has been used for the modification of electrode and applied for electrochemical determination, owing to its versatility and easiness of the preparation [29,30]. Thus, we report a facile one-step electrochemical method to prepare the poly(L-Arg)/graphene

* Corresponding author. Tel.: +86 931 8911895; fax: +86 931 8912582.
*E-mail address:* wangcm@lzu.edu.cn (C. Wang).

0039-9140/$ – see front matter © 2012 Elsevier B.V. All rights reserved.
doi:10.1016/j.talanta.2012.02.041

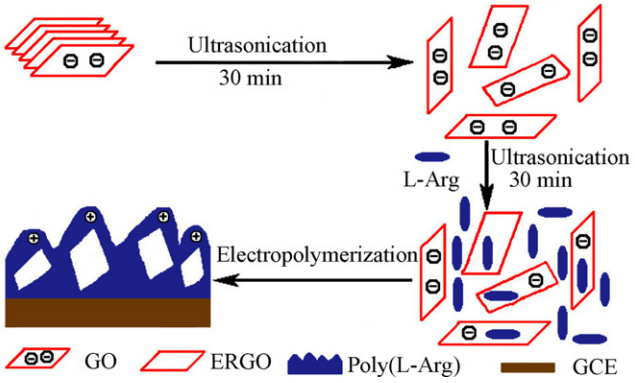


**Fig. 1.** Schematic illustration of the poly(L-Arg)/ERGO/GCE fabrication process.

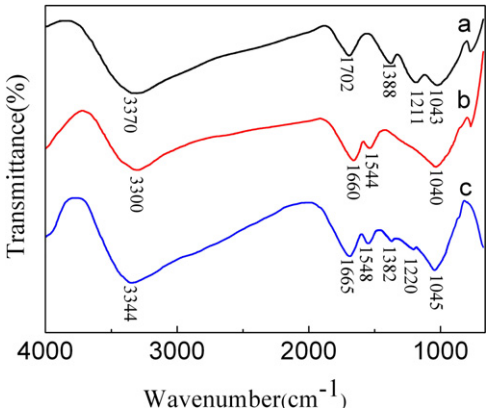


**Fig. 2.** FTIR spectra of GO (a), poly(L-Arg) (b), and poly(L-Arg)/ERGO (c).

composite film modified glass carbon electrode (GCE) for the first time. As illustrated in Fig. 1, electropolymerization of poly(L-Arg) and electrochemical reduction of GO (ERGO) were taken place simultaneously. The prepared new composite film possessed the advantages of both poly(L-Arg) and ERGO with a synergistic effect, which has excellent electrocatalytic activity for oxidation of UA, XA and HX with good sensitivity, wide linearity, high selectivity and remarkable reproducibility, which can be applied to determine these three compounds in human urine samples with satisfactory results.

## 2. Experimental

### 2.1. Chemicals

UA was purchased from Acros Orcanics. XA, HX and graphite flake (nature, −325 mesh) were purchased from Alfa Aesar. L-Arginine (L-Arg) was purchased from Sinopharm Chemical Reagent Co. Ltd. Freshly prepared solutions of UA, XA and HX were used in all experiments. The 0.10 M phosphate buffer solutions (PBS) with various pH values were prepared by mixing the stock solutions of 0.10 M $NaH_2PO_4$ and $Na_2HPO_4$ and adjusting the pH with 0.1 M NaOH and 0.1 M $H_3PO_4$. All chemicals were of analytical grade and were used without further purification. All solutions were prepared with doubly distilled water, purified by the Milli-Q system (Millipore Inc., 18.2 MΩ cm). GO was prepared from graphite powder by a modified Hummers method [31].

### 2.2. Apparatus and characterizations

Electrochemical measurements were performed on a CHI 822b workstation (Shanghai Chenhua, China) with a conventional three-electrode system. The bare or modified GCE (3.0 mm in diameter) was used as working electrode, platinum electrode as auxiliary electrode and saturated calomel electrode (SCE) as reference electrode. All pH measurements were performed using a pHs-3B digital pH-meter (Shanghai Lei Ci Device Works, Shanghai, China). The morphology of the samples was observed using field-emission scanning electron microscopy (FESEM, JSM-6701F, Kevex, Japan). Fourier transform infrared (FTIR) spectra were recorded on a NEXUS 670 FT-IR spectrometer (America).

### 2.3. Preparation of poly(L-Arg)/ERGO/GCE

Cyclic voltammetry (CV) was used to prepare the composite film. Prior to its modification, the bare GCE was polished with 0.3 and 0.05 μm alumina slurry, and sonicated in ethanol and water successively. To prepare the solution for poly(L-Arg)/ERGO film, 1 mg $ml^{-1}$ GO in 0.1 M PBS (pH 6.0) was ultrasonicated for 30 min, then appropriate amount of L-Arg was added to form an aqueous solution (10 μM), followed by ultrasonication for another 30 min. Finally, the polymeric film was electropolymerized by cyclic sweeping from −2.3 to 2.5 V at 100 mV $s^{-1}$ for 7 cycles. After polymerization, the modified electrode was washed with doubly distilled water, and then air-dried. For a comparison, poly(L-Arg) film without ERGO was also fabricated in 0.1 M PBS (pH 6.0) with 10 μM L-Arg.

## 3. Results and discussion

### 3.1. Characterizations of poly(L-Arg)/ERGO composite film

The FTIR spectra for the pristine GO, poly(L-Arg) and poly(L-Arg)/ERGO are shown in Fig. 2. The FTIR spectrum of GO shows a broad and intense peak centered at 3370 $cm^{-1}$ and a peak at 1702 $cm^{-1}$, corresponding to the O—H groups and the carbonyl (C=O) stretching vibration, respectively. The peaks at 1388, 1211 and 1043 $cm^{-1}$ are assigned to the O—H deformation vibration, the carboxyl (C—OH) and alkoxy (C—O) groups stretching vibration, respectively (Fig. 2(a)) [32]. In the poly(L-Arg), the peak at 1660 $cm^{-1}$ is assigned to amide I (C=O carbonyl stretch and guanidine (C=N) stretch), the peak at 1544 $cm^{-1}$ is assigned to amide II (C=N stretch and N—H bending), the peaks at 1040 and 3300 $cm^{-1}$ are assigned to the C—N and N—H stretching vibration, respectively (Fig. 2(b)) [33,34]. In the poly(L-Arg)/ERGO composite, characteristic peaks of poly(L-Arg) can be found, furthermore, the absence of the peaks at 1702 $cm^{-1}$ and the decrease of the peak intensity at 1220 and 1382 $cm^{-1}$ indicate that GO has been reduced to ERGO. These results suggest that GO not only could be electrochemically reduced to ERGO but also simultaneously successfully incorporated into the poly(L-Arg) film.

Compared with the bare GCE, the electropolymerized ploy (L-Arg) film and poly(L-Arg)/ERGO film show colorful color (insets of Fig. 3), indicating the films have been successfully adhered to the electrode surface. It can be clearly seen that the poly(L-Arg) film is very smooth, uniform and dense comparing to bare GCE (Fig. 3A and B). When GO was added into the deposition solution, poly(L-Arg)/ERGO film shows a rough surface feature with nanometer-scale bulges compared with pure poly(L-Arg) film in Fig. 3C, which indicates that the ERGO were completely embedded into the polymer structure and enhanced the specific surface area of the film. In addition, the electrochemically effective surface areas (A) of poly(L-Arg)/GCE and poly(L-Arg)/ERGO/GCE were investigated by chronocoulometry (Fig. S1 in Supplementary material). A was calculated to be 0.033 $cm^2$ for poly(L-Arg)/GCE and 0.048 $cm^2$ for poly(L-Arg)/ERGO/GCE, indicating that the introduced ERGO enhanced the effective surface areas of the film.

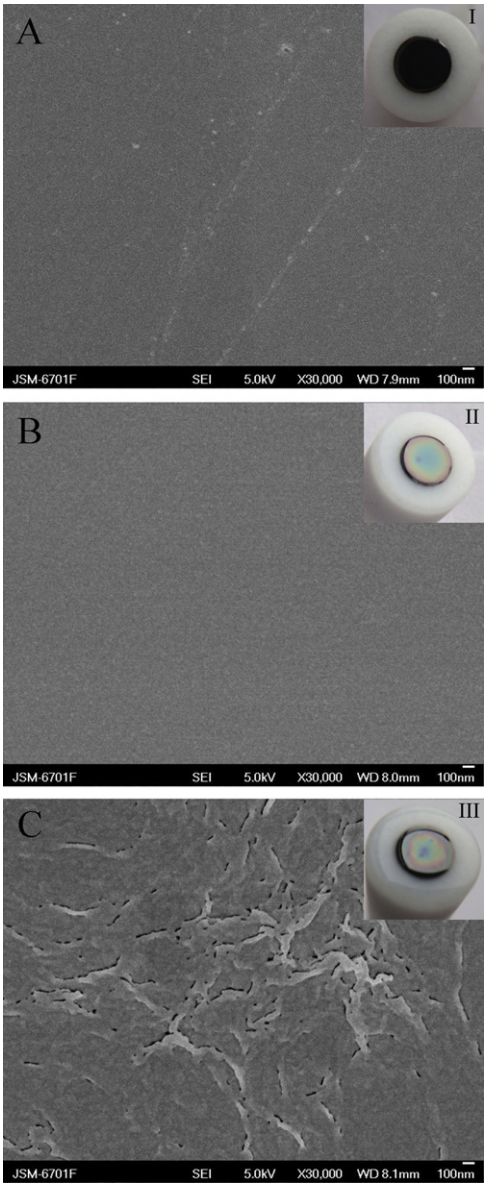


**Fig. 3.** FESEM images of bare GCE (A), poly(L-Arg) film (B), and poly(L-Arg)/ERGO film (C). The insets I, II and III are the photos of the bare GCE GO, poly(L-Arg)/GCE and poly(L-Arg)/ERGO/GCE, respectively.

### 3.2. Voltammetric behavior of UA, XA and HX at different electrodes

Fig. 4 shows CV responses of the mixture solution containing 50 μM UA, XA and HX at bare GCE and modified electrode in pH 6.5 PBS. The oxidation peak currents and potentials of different electrodes are listed in Table 1. It is found that the oxidation peak currents ($i_{pa}$) of UA, XA and HX at poly(L-Arg)/GCE are 2.1, 4.4 and 2.7 times as high as those at the bare GCE, respectively. Above experimental data confirmed that poly(L-Arg) had a great electrochemical activity for UA, XA and HX oxidation compared to bare GCE. The poly(L-Arg)/ERGO/GCE shows the largest oxidation peak currents, which are 6.0, 8.9 and 5.3 times as high as those at the bare GCE, respectively. In addition, all the three oxidation peak potentials on poly(L-Arg)/ERGO/GCE shift slightly to more negative potential compared to bare GCE. These results might be attributed to the synergistic effect of poly(L-Arg) and ERGO, in which poly(L-Arg) has electrocatalytic ability for three compounds

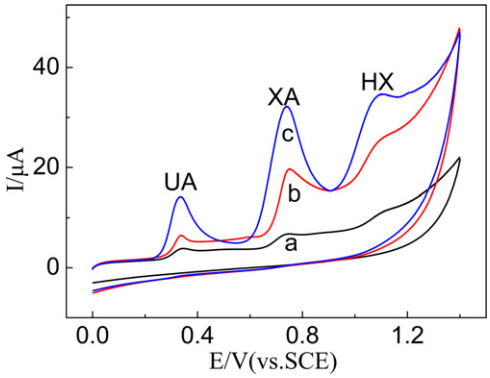


**Fig. 4.** CVs of bare GCE (a), poly(L-Arg)/GCE (b), and poly(L-Arg)/ERGO/GCE (c) in 0.1 M PBS (pH = 6.5) containing 50 μM UA, XA and HX solutions with a scan rate of 50 mV $s^{-1}$.

and the ERGO provide a large specific surface area. Meanwhile, ERGO could accelerate the electron transfer on the electrode surface to amplify the electrochemical signal due to its excellent electric conductivity.

### 3.3. Effect of scan rate on the oxidation of UA, XA and HX at poly(L-Arg)/ERGO/GCE

The kinetics of the electrode reactions was investigated by studying the effects of scan rate on the peak currents. Fig. 5A shows the CVs of 50 μM UA, XA and HX mixture solution on the

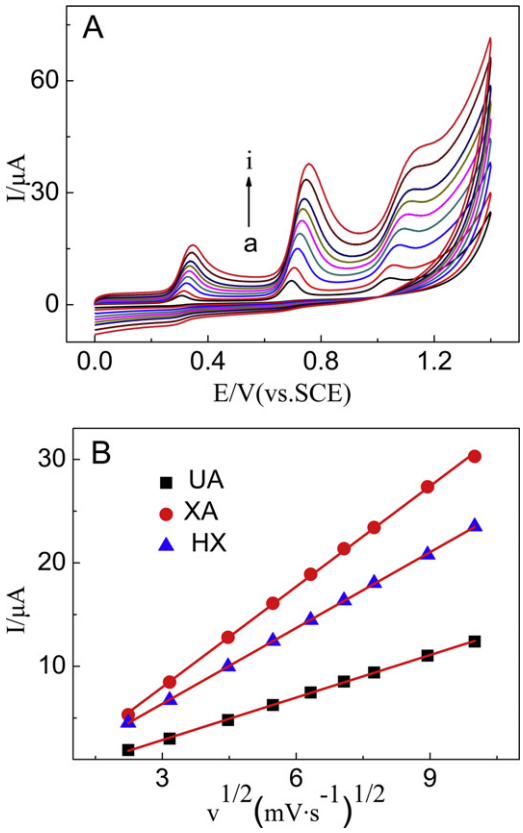


**Fig. 5.** (A) CVs of 50 μM UA, XA and HX mixture solution on the poly(L-Arg)/ERGO/GCE at different scan rates (a–i: 5, 10, 20, 30, 40, 50, 60, 80, 100 mV $s^{-1}$) in 0.1 M PBS (pH = 6.5). (B) Plots of the oxidation peak current versus the square root of scan rate.

**Table 1**
Detailed data of cyclic voltammograms at different electrodes.

| Electrode | UA | | X | | Hx | |
|---|---|---|---|---|---|---|
| | $i_{pa}$ (μA) | $E_{pa}$ (V) | $i_{pa}$ (μA) | $E_{pa}$ (V) | $i_{pa}$ (μA) | $E_{pa}$ (V) |
| Bare GCE | 2.05 | 0.345 | 3.05 | 0.753 | 3.66 | 1.11 |
| Poly(L-Arg)/GCE | 4.35 | 0.343 | 13.5 | 0.751 | 9.74 | 1.10 |
| Poly(L-Arg)/ERGO/GCE | 12.3 | 0.338 | 27.2 | 0.747 | 19.5 | 1.09 |

poly(L-Arg)/ERGO/GCE at different scan rates. With the increase of the scan rate, the oxidation peak currents increased simultaneously. The plots of oxidation peak currents as a function of scan rate for three molecules were also shown in the insets of Fig. 5B. In the range from 5 to 100 mV $s^{-1}$, the oxidation peak currents increase linearly with the square root of the scan rate (the linear regression equations are $i_{pa}(\mu A) = 1.370v^{1/2} - 1.236$ for UA with a correlation coefficient of $R^2 = 0.9997$, $i_{pa}(\mu A) = 3.238v^{1/2} - 1.724$ ($R^2 = 0.9995$) for XA, and $i_{pa}(\mu A) = 2.442v^{1/2} - 0.9513$ ($R^2 = 0.9999$) for HX, respectively), which suggest that the system presents features corresponding to a diffusion-controlled process for UA, XA and HX.

### 3.4. Effect of pH value on the oxidation of UA, XA and HX at the modified electrode

The pH value of the supporting electrolyte has a significant influence in the simultaneous determination of UA, XA and HX, by varying both the peak potential and peak current. Fig. 6 illustrated the dependence of the anodic peak potential ($E_{pa}$) and anodic peak current ($i_{pa}$) for 50 μM UA, XA and HX on pH of buffer solution. The peak potentials ($E_{pa}$) for UA, XA and HX showed a same trend and shift almost linearly toward negative potentials when pH was increased in the range of 2.5–10.5, indicating that protons are directly involved in the rate determination step of the oxidation reaction of the three species. The equation relating $E_{pa}$ with pH was found to be: $E_{pa}(mV) = 1505 - 63.7pH$ ($R^2 = 0.9962$) for HX, $E_{pa}(mV) = 1151 - 63.2pH$ ($R^2 = 0.9988$) for XA, and $E_{pa}(mV) = 744.3 - 63.1pH$ ($R^2 = 0.9994$) for UA, respectively. The slopes of $-63.7$ mV $pH^{-1}$ for HX, $-63.2$ mV $pH^{-1}$ for XA, and $-63.1$ mV $pH^{-1}$ for UA are close to the theoretical value of $-59.0$ mV $pH^{-1}$ which indicates that two protons and two electrons are involved in oxidation process. This is in agreement with literature reported in [17,18]. The effect of pH on anodic peak current for UA, XA and HX was shown in Fig. 6B. It could be seen that the maximum value appeared at pH 6.5 for the three species. Therefore, considering the sensitivity, 0.1 M PBS (pH = 6.5) was chosen as supporting electrolyte for the simultaneous determination of UA, XA and HX in this study.

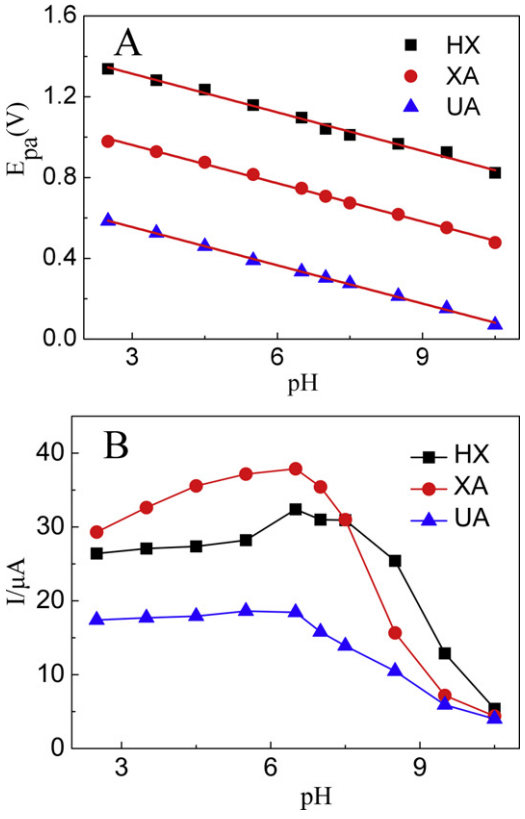


**Fig. 6.** Effects of pH on the anodic peak potential (A) and anodic peak current (B) of 50 μM UA, XA and HX at poly(L-Arg)/ERGO/GCE, respectively. Scan rate: 50 mV $s^{-1}$, 0.1 M PBS.

### 3.5. Simultaneous determination of UA, XA and HX

Since differential pulse voltammetry (DPV) has higher current sensitivity and better resolution than CV, it was used for simultaneous determination of UA, XA and HX. Fig. 7 shows the DPV response at the modified electrode while synchronously varying the concentration of UA, XA and HX. The results showed that the peak currents of DPV are linearly proportional to the concentrations of the three compounds, respectively. The linear ranges and detection limits of UA, XA and HX were shown in Table 2, respectively. Furthermore, the comparison of this method with other electrochemical methods for the simultaneous determination of UA, XA and HX was listed in Table 3. It can be observed that the linear range and detection limit for poly(L-Arg)/ERGO/GCE are comparable and even better than those obtained at several electrodes reported recently.

### 3.6. Interference study

For evaluating selectivity of the poly(L-Arg)/ERGO modified electrode, various possible interfering species were examined for their effect on the determination of UA, XA and HX (all of them were 5.0 μM). The results are listed in Table 4. Under the existence of those species, the recovery of UA, XA and HX changed between 95.7% and 106.7%, which indicates that those interferents have no interference at high concentrations.

### 3.7. Reproducibility of the modified electrode

In order to test the repeatability of the poly(L-Arg)/ERGO modified electrode, the DPVs for 2.5 μM UA, XA and 5 μM HX in 0.1 M PBS (pH 6.5) solution were determined repeatedly at the identical surface of poly(L-Arg)/ERGO/GCE successive 10 times. The relative standard deviations (RSD) of the peak currents for UA, XA and HX were 2.0%, 1.3% and 2.5%, respectively. The same solutions were also determined with 10 modified electrodes made independently, and the RSD for peak currents of UA, XA and HX were 2.2%, 1.6% and

**Table 2**
Analytical characteristics for simultaneous determination of UA, XA and HX.

| Analyte | Linear range (μM) | Linear regression equation ($i$: μA, $C$: μM) | Correlation coefficient | Detection limit (μM) |
|---|---|---|---|---|
| UA | 0.10–10.0 | $i_{pa} = 0.3873C + 0.1654$ | 0.9977 | 0.05 |
| XA | 0.10–10.0 | $i_{pa} = 0.5362C + 0.1204$ | 0.9967 | 0.05 |
| HX | 0.20–20.0 | $i_{pa} = 0.2007C + 0.0468$ | 0.9959 | 0.10 |

1.6%, respectively. Furthermore, when the poly(L-Arg)/ERGO/GCE was stored at room temperature for one week, the current response to 2.5 μM UA, XA and 5 μM HX remained 92.9%, 93.1% and 93.4% of their original values, respectively, suggesting the long-term stability of the electrode. So the modified electrode possesses remarkable reproducibility, excellent precision and long-term stability.

### 3.8. Analytical applications

The practical analytical utility of the modified electrode was illustrated by simultaneous determination of UA, XA and HX in human urine samples. The human urine samples were collected from laboratory co-workers. Because the content of HX in human urine was lower than the detection limits of this method, the real samples were spiked with certain amounts of HX. After all the urine samples were diluted 1000-fold with pH 6.5 PBS, the three compounds were determined simultaneously by the proposed DPV method. The obtained results were summarized in Table 5. It can be seen that all spike recoveries were accurate and precise, which indicated the good applicability of the poly(L-Arg)/ERGO modified electrode to simultaneous determination of UA, XA and HX in the real samples. In addition, in order to ascertain the accuracy of the proposed method, the analytical results of UA in human urine samples applied by the modified electrode were compared with those obtained by the standard enzymatic method (Table S1 in Supplementary material). The analytical results suggested that the proposed method is reliable.

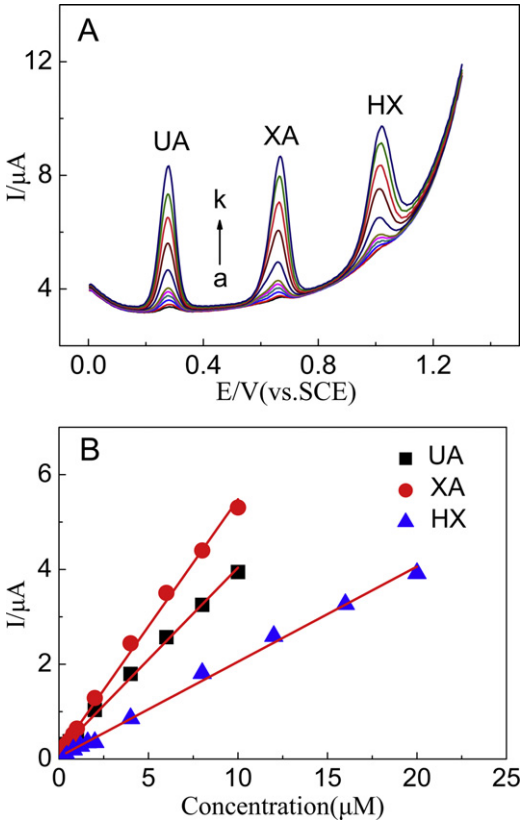


**Fig. 7.** (A) DPV of different concentrations of UA, XA (a → k: 0.1, 0.2, 0.4, 0.6, 0.8, 1.0, 2.0, 4.0, 6.0, 8.0, 10 μM) and HX (a → k: 0.2, 0.4, 0.8, 1.2, 1.6, 2.0, 4.0, 8.0, 12.0, 16.0, 20.0 μM) on the poly(L-Arg)/ERGO/GCE in 0.1 M PBS pH 6.5. (B) Concentration calibration curve of the DPV current response for UA, XA and HX.

**Table 3**
Comparison of the proposed method with other electrochemical methods for the simultaneous determination of UA, XA and HX.

| Electrode | Linear range (μM) | Detection limit (μM) | Ref. |
|---|---|---|---|
| Preanodized nontronite coated screen-printed carbon electrode | UA: 2–40<br>XA: 2–40<br>HX: 4–30 | UA: 0.42<br>XA: 0.07<br>HX: 0.32 | [13] |
| Inlaying ultra-thin carbon paste electrode modified with functional single-wall carbon nanotubes | UA: 0.1–100<br>XA: 0.2–100<br>HX: 0.8–100 | UA: 0.08<br>XA: 0.146<br>HX: 0.562 | [14] |
| $Ru(DMSO)_4Cl_2$ nano-aggregated Nafion membrane modified electrode | UA: 100–700<br>XA: 50–500<br>HX: 50–300 | UA: 0.372<br>XA: 2.35<br>HX: 2.37 | [15] |
| Poly(BCP) modified glassy carbon electrode | UA: 0.5–120<br>XA: 0.1–100<br>HX: 0.2–80 | UA: 0.2<br>XA: 0.06<br>HX: 0.12 | [17] |
| A nanostructured polymer film modified electrode | AA: 30–300<br>DA: 5–50<br>UA: 10–100<br>XA: 10–100 | AA: 2.01<br>DA: 0.33<br>UX: 0.19<br>XA: 0.59 | [18] |
| Poly(L-arginine)/graphene composite film modified electrode | UA: 0.1–10<br>XA: 0.1–10<br>HX: 0.2–20 | UA: 0.05<br>XA: 0.05<br>HX: 0.10 | This work |

**Table 4**
Interferences of some foreign substances for 5.0 μM UA, XA and HX.

| Interferents | Interferents concentration (μM) | Recovery (%) | | |
|---|---|---|---|---|
| | | UA | XA | HX |
| Glucose | 2500 | 101.7 | 102.4 | 98.1 |
| Citrate | 2500 | 106.7 | 104.0 | 96.3 |
| Cysteine | 500 | 97.3 | 101.1 | 100.5 |
| Serine | 500 | 98.9 | 101.7 | 100.2 |
| Ascorbic acid | 100 | 100.2 | 104.6 | 95.7 |
| Dopamine | 250 | 98.2 | 106.3 | 97.0 |
| Oxalic acid | 250 | 99.3 | 106.0 | 101.3 |
| Urea | 1000 | 97.6 | 99.5 | 98.1 |
| Uracil | 100 | 98.7 | 104.5 | 99.9 |
| Thiourea | 250 | 103.9 | 104.6 | 99.3 |
| Histidine | 300 | 96.9 | 103.6 | 102.6 |
| Adenosine | 50 | 97.1 | 98.6 | 103.2 |

**Table 5**
Simultaneous determination of UA, XA and HX in human urine samples ($n = 3$).

| Samples | Original (μM) | | | Added (μM) | | | Found (μM) | | | Recoveries (%) | | |
|---|---|---|---|---|---|---|---|---|---|---|---|---|
| | UA | XA | HX | UA | XA | HX | UA | XA | HX | UA | XA | HX |
| Urine 1 | 3.39 | 0.61 | – | 0.50 | 0.50 | 0.50 | 3.91 | 1.15 | 0.47 | 104.0 | 108.0 | 94.0 |
| Urine 2 | 3.35 | 0.54 | – | 0.50 | 0.50 | 0.50 | 3.83 | 1.07 | 0.51 | 96.0 | 106.0 | 102.0 |
| Urine 3 | 2.36 | 0.22 | – | 0.50 | 0.50 | 0.50 | 2.84 | 0.74 | 0.48 | 96.0 | 104.0 | 96.0 |
| Urine 4 | 2.09 | 0.46 | – | 0.50 | 0.50 | 0.50 | 2.63 | 1.00 | 0.49 | 108.0 | 108.0 | 98.0 |
| Urine 5 | 2.80 | 0.43 | – | 0.50 | 0.50 | 0.50 | 3.27 | 0.96 | 0.47 | 94.0 | 106.0 | 94.0 |

## 4. Conclusions

In this paper, poly(L-Arg)/graphene composite film modified electrode has been developed through a facile, green and one-step electropolymerization process from GO and L-Arg precursors, and used for simultaneous determination of UA, XA and HX by DPV. The poly(L-Arg)/ERGO modified electrode possesses good stability, excellent sensitivity and high selectivity for simultaneous detection of UA, XA and HX. In addition, the modified electrode also has good reproducibility and can be applied to determination of purine derivatives in human urine samples with satisfactory results. Hence, the poly(L-Arg)/ERGO modified electrode is a potential useful tool for the assay of UA, XA and HX both in research assays and clinical diagnosis due to its fast, precisely and inexpensive features.

## Acknowledgment

This work is financially supported by the National Nature Science Foundation of China (NO. 20775030).

## Appendix A. Supplementary data

Supplementary data associated with this article can be found, in the online version, at doi:10.1016/j.talanta.2012.02.041.

## References

[1] T. Yamamoto, Y. Moriwaki, S. Takahashi, Clin. Chim. Acta 356 (2005) 35–57.
[2] M. Heinig, R.J. Johnson, Cleve. Clin. J. Med. 73 (2006) 1059–1064.
[3] M.A. Carsol, G. Volpe, M. Mascini, Talanta 44 (1997) 2151–2159.
[4] E.E. Kelley, A. Trostchansky, H. Rubbo, B.A. Freeman, R. Radi, M.M. Tarpey, J. Biol. Chem. 279 (2004) 37231–37234.
[5] M. Czauderna, J. Kowalczyk, J. Chromatogr. B: Biomed. Sci. Appl. 744 (2000) 129–138.
[6] M. Czauderna, J. Kowalczy, J. Chromatogr. B: Biomed. Sci. Appl. 704 (1997) 89–98.
[7] N. Cooper, R. Khosravan, C. Erdmann, J. Fiene, J.W. Lee, J. Chromatogr. B 837 (2006) 1–10.
[8] L. Terzuoli, B. Porcelli, C. Setacci, M. Guibbolini, J. Chromatogr. B: Biomed. Sci. Appl. 728 (1999) 185–192.
[9] E. Caussé, A. Pradelles, B. Dirat, A. Negre-Salvayre, R. Salvayre, F. Couderc, Electrohporesis 28 (2007) 381–387.
[10] F. Carlucci, A. Tabucchi, B. Biagioli, G. Sani, G. Lisi, M. Maccherini, F. Rosi, E. Marinello, Electrophoresis 21 (2000) 1552–1557.
[11] M. Cubukcu, S. Timur, U. Anik, Talanta 74 (2007) 434–439.
[12] X. Cai, K. Kalcher, C. Neuhold, Fresenius J. Anal. Chem. 348 (1994) 660–665.
[13] J.M Zen, Y.Y. Lai, H.H. Yang, A. Senthil Kumar, Sens. Actuators B: Chem. 84 (2002) 237–244.
[14] Z.H. Wang, X.Y. Dong, J. Li, Sens. Actuators B: Chem. 131 (2008) 411–416.
[15] A.S. Kumar, P. Swetha, J. Electroanal. Chem. 642 (2010) 135–142.
[16] R.N. Goyal, A. Mittal, S. Sharma, Electroanalysis 6 (1994) 609–611.
[17] Y. Wang, L.L. Tong, Sens. Actuators B 150 (2010) 43–49.
[18] P. Kalimuthu, S.A. John, Talanta 80 (2010) 1686–1691.
[19] K.S. Novoselov, A.K. Geim, S.V. Morozov, D. Jiang, Y. Zhang, S.V. Dubonos, I.V. Grigorieva, A.A. Firsov, Science 306 (2004) 666–669.
[20] S. Stankovich, D.A. Dikin, G.H.B. Dommett, K.M. Kohlhaas, E.J. Zimney, E.A. Stach, R.D. Piner, S.T. Nguyen, R.S. Ruoff, Nature 442 (2006) 282–286.
[21] Y.M. Lin, C. Dimitrakopoulos, K.A. Jenkins, D.B. Farmer, H.Y. Chiu, A. Grill, P. Avouris, Science 327 (2010) 662.
[22] J.S. Bunch, A.M. van der Zande, S.S. Verbridge, I.W. Frank, D.M. Tanenbaum, J.M. Parpia, H.G. Craighead, P.L. McEuen, Science 315 (2007) 490–493.
[23] K.V. Emtsev, A. Bostwick, K. Horn, J. Jobst, G.L. Kellogg, L. Ley, J.L. McChesney, T. Ohta, S.A. Reshanov, J. Rohrl, E. Rotenberg, A.K. Schmid, D. Waldmann, H.B. Weber, T. Seyller, Nat. Mater. 8 (2009) 203–207.
[24] G. Chen, W. Weng, D. Wu, C. Wu, J. Lu, P. Wang, X. Chen, Carbon 42 (2004) 753–759.
[25] S. Stankovich, R.D. Piner, X.Q. Chen, N.Q. Wu, S.T. Nguyen, R.S. Ruoff, J. Mater. Chem. 16 (2006) 155–158.
[26] S. Stankovich, D.A. Dikin, R.D. Piner, K.A. Kohlhaas, A. Kleinhammes, Y.Y. Jia, Y. Wu, S.T. Nguyen, R.S. Ruoff, Carbon 45 (2007) 1558–1565.
[27] H.C. Gao, F. Xiao, C.B. Ching, H.W. Duan, ACS Appl. Mater. Interfaces 3 (2011) 3049–3057.
[28] H.L. Guo, X.F. Wang, Q.Y. Qian, F.B. Wang, X.H. Xia, ACS Nano 3 (2009) 2653–2659.
[29] W. Ma, D.M. Sun, Chin. J. Anal. Chem. 35 (1) (2007) 66–70.
[30] Q. Cao, H. Zhao, Y.M. Yang, Y.J. He, N. Ding, J. Wang, Z.J. Wu, K.X. Xiang, G.W. Wang, Biosens. Bioelectron. 26 (2011) 3469–3474.
[31] S. Gilje, S. Han, M.S. Wang, K.L. Wang, R.B Kaner, Nano Lett. 7 (2007) 3394–3398.
[32] Y.X. Xu, H. Bai, G.W. Lu, C. Li, G.Q. Shi, J. Am. Chem. Soc. 130 (2008) 5856–5857.
[33] Sérgio V.P. Barreira, F. Silva, Langmuir 19 (2003) 10324–10331.
[34] P. Sharma, N.K. Misra, P. Tandon, V.D. Gupta, J. Macromol. Sci. B 41 (2) (2002) 319–340.